Nuclear Physics B 386 (1992) 495–519
North-Holland

NUCLEAR
PHYSICS B

Quantum field theoretic behavior of a deterministic cellular automaton

G. 't Hooft, K. Isler and S. Kalitzin [1]

Institute for Theoretical Physics, Princetonplein 5, P.O. Box 80.006, 3508 TA Utrecht, The Netherlands

Received 22 June 1992
Accepted for publication 28 August 1992

A certain class of cellular automata in 1 space +1 time dimension is shown to be closely related to quantum field theories containing Dirac fermions. In the massless case this relation can be studied analytically, while the introduction of Dirac mass requires numerical simulations. We show that in the last case the cellular automaton describes the corresponding field theory only approximately.

1. Introduction

A cellular automaton is a large array of elements or "cells", usually situated on a one or more dimensional lattice; at each cell one or several dynamical variables (we will call them *spins*) can take a finite number of different values. At each tick of an external clock the contents of all cells are updated according to some law of evolution. For each particular cell this law may be very simple, involving only its nearest neighbors besides itself. The system as a whole can then behave in a very complex way, and it is ideally suited for computer investigations.

The automata considered in this paper are [1] *deterministic*, which means that there is no random number generator in the local law of evolution, and *time reversible*, which means that any configuration can be extrapolated backwards in time as easily as forward in time. We consider in this paper only the simplest type automata – the boolean ones. Such an automaton comprises a set of cells σ_i, $i = 1, \ldots, N$, each taking two values 0 or 1. The state of the automaton, σ, is defined by the values of all cells.

To apply the concept of cellular automata evolution to the field theoretical models we exploit the philosophy explained by one of the authors in earlier papers [2]. We start by introducing a *Hilbert space* such that each state σ of our

[1] On leave from Inst. Nucl. Res. Nuclear Energy, bul Trakia 72, Sofia 1184, Bulgaria.

0550-3213/92/$05.00 © 1992 – Elsevier Science Publishers B.V. All rights reserved

automaton corresponds to a *basis element* $|\sigma\rangle$. So for an arbitrary vector $|\psi\rangle$ (a superposition of $|\sigma\rangle$) we can define the probability of a given state σ as

$$P(\sigma) = |\langle\sigma|\psi\rangle|^2. \tag{1.1}$$

At this point it will be clear that the phase angles in these state vectors are spurious; we may choose them any way we like. However, we will discover that there are ways to reproduce the evolution of σ by writing down a Schrödinger equation for ψ:

$$\frac{\mathrm{d}}{\mathrm{d}t}|\psi\rangle = -iH|\psi\rangle. \tag{1.2}$$

At *integer* time t any basis element σ evolves into $\sigma(t)$ in accordance to the law of the cellular automaton. But this equation now also prescribes how the phase factors evolve.

There are many different choices for H that all reproduce the same cellular automaton, but only a small subclass of these are *extensive*:

$$H = \sum_x \mathscr{H}(x), \tag{1.3}$$

where $\mathscr{H}(x)$ is a hamiltonian *density*. It is hamiltonians of the kind (1.3) that would correspond to genuine quantum field theories. Once we choose our hamiltonian to be of this form we discover two things: first, techniques of quantum field theory can be used to describe phenomena at distance scales much larger than the lattice length, and secondly, phase factors among states become physically important. Thus, quantum mechanical phase factors are crucially linked to the decomposability (1.3) of the hamiltonian.

We will also see however that (1.3) cannot be exactly true in most cases. The Hamilton density $\mathscr{H}(x)$ cannot be completely local, i.e. depend only on x and its direct neighbors. What will happen is that $\mathscr{H}(x)$ is an infinite sum, whose successive terms involve interactions among increasingly distant neighbors. This forces us to limit ourselves to only a subclass of all states $|\psi\rangle$, namely those for which the summation for $\mathscr{H}(x)$ converges sufficiently rapidly. In general, the states $|\psi\rangle$, $|\varphi\rangle$, for which the matrix elements $\langle\psi|\mathscr{H}(x)|\psi\rangle$ converge rapidly are those states for which the total energy E is close to the vacuum value: $|E - E_0| \ll 2\pi$ (in natural units).

From the point of view of quantum field theory this constraint is only natural: we should not allow for too energetic particle configurations; to describe those one has to go back to the complete description of the original cellular automaton.

But if one wants to check our claims with computer simulations this condition is very difficult; one never knows whether the initial state corresponds to particles

with sufficiently low total energy; indeed, one starts to work with the basis elements $|\sigma\rangle$, for which of course the constraint does not hold. One then has to introduce large ensembles and compute averages.

In practice also another problem shows up: it is very difficult to devise a hamiltonian in such a way that it does not fluctuate somewhat between two time steps. As soon as our hamiltonian has such a periodic time dependence one may expect violation of energy conservation that gives rise to spontaneous generation of "energetic showers" of a kind not wanted in a realistic field theoretical model. This may explain why our attempts at computer simulations, to be explained later, sometimes give unexpected results.

The paper is organized as follows. In sect. 2 we present a particular automaton evolution and build the corresponding Hilbert space. We also show that in the continuum limit this quantum system reproduces exactly the massless Fermi field theory. Sect. 3 is devoted to an attempt to perturb the evolution rule for the automaton in order to obtain the massive Dirac theory in the continuum limit. The analytical calculations for the last case are presented in sect. 4 and the numerical emulations for this automaton are discussed in sect. 5.

2. The one-dimensional shift automaton

The automaton to be considered first is physically very trivial, but useful to elucidate our techniques. Divide the circle into N cells. In each cell x a spin σ_x can take the values 0 and 1. The evolution equation is taken to be

$$\sigma_{x,t+1} = \sigma_{x-1,t}, \qquad \sigma_{N,t} = \sigma_{0,t} \tag{2.1}$$

or, in other words, the spins shift to the right at constant speed.

The Hilbert space has 2^N dimensions; it is spanned by the basis elements $\{|\sigma_1, \sigma_2, \ldots, \sigma_N\rangle\}$. We can introduce the Pauli matrices τ_x^a, $a = 1, 2, 3$, at each site x. They obey

$$\left[\tau_x^a, \tau_y^b\right] = 2i\delta_{xy}\varepsilon^{abc}\tau_x^c. \tag{2.2}$$

We write

$$\sigma_x = \tau_x^+\tau_x^- . \tag{2.3}$$

If N is odd, $N = 2n + 1$, we can perform a Jordan–Wigner transformation as follows:

$$\psi_x = \tau_{x-n}^3 \otimes \tau_{x-n+1}^3 \otimes \ldots \otimes \tau_{x-1}^3 \otimes \tau_x^- \otimes \mathbb{I}_{x+1} \otimes \ldots \otimes \mathbb{I}_{x+n}, \tag{2.4}$$

so that

$$\{\psi_x^\dagger, \psi_y\} = \delta_{xy}, \qquad \{\psi_x, \psi_y\} = 0, \tag{2.5}$$

$$\psi_{x,t} = \psi_{x-t,0}. \tag{2.6}$$

This allows us, in a standard way, to perform the discrete Fourier transform:

$$\hat{\psi}_p = N^{-1/2} \sum_x \omega^{-px} \psi_x, \quad \omega = e^{2\pi i/N}, \tag{2.7}$$

such that

$$\{\hat{\psi}_p^\dagger, \hat{\psi}_q\} = \delta_{pq}, \qquad \{\hat{\psi}_p, \hat{\psi}_q\} = 0. \tag{2.8}$$

The time evolution of $\hat{\psi}_p$ is then

$$\hat{\psi}_{p,t} = U^\dagger(t)\hat{\psi}_{p,0}U(t) = \omega^{-pt}\psi_{p,0}. \tag{2.9}$$

We can therefore take as our hamiltonian

$$H = \frac{2\pi}{N} \sum_{p=-n}^{n} p\hat{\psi}_p^\dagger \hat{\psi}_p + \text{const.}, \qquad U(t) = e^{-iHt}, \tag{2.10}$$

where the constant is chosen such that the lowest energy level is zero. In the above case it is $\pi n(n+1)/N$. This corresponds to normal ordering of the operators $\hat{\psi}_p$ with respect to the lowest energy state.

To take the continuum limit of (2.10) we proceed in two steps. First we obtain the infinite-volume limit $N \to \infty$ of (2.10) in x-space, which is

$$H = \sum_{x \neq y} \frac{(-1)^{(x-y)}}{x-y} :\psi_x^\dagger \psi_y :, \qquad x, y = -\infty \ldots +\infty.$$

Next we go to the compact momentum space and obtain the expression

$$H = \int_{-\pi}^{\pi} \mathrm{d}p\, p :\hat{\psi}_p^\dagger \hat{\psi}_p :.$$

After rescaling the momenta $p \to \Lambda p$ and field operators $\psi \to \psi/\sqrt{\Lambda}$, the hamiltonian obeys in the limit $\Lambda \to \infty$ the condition (1.3):

$$H \to \sum_x \mathscr{H}(x), \qquad \mathscr{H}(x) \to -i :\psi_x^\dagger \partial_x \psi_x :, \tag{2.11}$$

while in the discrete system ∂_x is replaced by an infinite series of finite displacement operators (from the Fourier transform of p in (2.10)). For our purposes H is sufficient local to apply quantum field theory. For more on the continuum limit see below.

Notice also that the choice (2.10) is not unique; we could for instance have chosen the boundaries $-n$, n different.

In quantum field theory the hamiltonian (2.11) is recognized to be the one describing massless, chiral Dirac fermions. The lowest-energy state of (2.10), the *vacuum state* $|0\rangle$, is then defined by

$$\left.\begin{aligned} \hat{\psi}_p^\dagger |0\rangle &= 0 \quad (p \leqslant -1) \\ \hat{\psi}_p |0\rangle &= 0 \quad (p \geqslant 0) \end{aligned}\right\} \Rightarrow |0\rangle = \hat{\psi}^\dagger_{-n} \ldots \hat{\psi}^\dagger_{-1} |\sigma = 0\rangle. \tag{2.12}$$

This state is obviously stationary in time. What are the corresponding $P(\sigma)$?

To compute these we must Fourier transform back to x-space:

$$\begin{aligned} |0\rangle &= N^{-n/2} \prod_{p<0} \left(\sum_{X_p=-n}^{n} \omega^{px_p} \psi^\dagger_{x_p} \right) |\sigma = 0\rangle \\ &= N^{-n/2} \sum_{\{x_1,\ldots,x_n\}} \omega^{x_1} \omega^{2x_2} \ldots \omega^{nx_n} \psi^\dagger_{x_1} \ldots \psi^\dagger_{x_n} |\sigma = 0\rangle \\ &= N^{-n/2} \sum_{x_1<x_2<\ldots<x_n} \sum_{\text{perm}} (-1)^{\text{perm}}\, \omega^{x_{P_1}+\ldots+nx_{P_n}} \psi^\dagger_{x_1} \ldots \psi^\dagger_{x_n} |\sigma = 0\rangle \\ &= N^{-n/2} \sum_{x_1<x_2<\ldots<x_n} \det_{(ij)} (\omega^{ix_j}) \, |x_1, \ldots x_n\rangle, \end{aligned} \tag{2.13}$$

where, up to a phase factor ± 1, the vector $|x_1, \ldots, x_n\rangle$ is the state with $\sigma = 1$ at the sites $x_1, \ldots, x_n$, and $\sigma = 0$ elsewhere.

The amplitude is the Van der Monde determinant:

$$\begin{aligned} A_{\{x_1,\ldots,x_n\}} &= N^{-n/2} \det \begin{pmatrix} 1 & \ldots & 1 \\ \omega^{x_1} & \ldots & \omega^{x_n} \\ \vdots & & \vdots \\ \omega^{(n-1)x_1} & \ldots & \omega^{(n-1)x_n} \end{pmatrix} \\ &= 2^{n(n-1)/2}\, N^{-n/2} \prod_{x_i<x_j} \sin \frac{\pi}{N} (x_i - x_j). \end{aligned} \tag{2.14}$$

We see that all allowed states have exactly n spins one and $n+1$ spins zero. Their probabilities are given by the square of (2.14). We can write these also as

$$A^2(x_1,\ldots,x_n) = C\,\exp\Big(2\sum_{i<j}\ln\,d_{ij}\Big), \tag{2.15}$$

with

$$d_{ij} = 2\,\sin\frac{\pi}{N}(x_i - x_j), \tag{2.16}$$

which happens to be the distance in two-dimensional space between the points x_i and x_j on the unit circle. Indeed, (2.15) is the Boltzmann factor of a two-dimensional Coulomb gas confined to the unit circle, at a certain temperature.

To compute correlation functions we can either use (2.15) directly or compute the vacuum expectation values of the corresponding operators using the expression (2.12) for our vacuum state.

For the two-point fermion correlation function, one finds in the limit $N\to\infty$:

$$\langle\psi_x^+\psi_y\rangle = \langle\psi_x\psi_y^+\rangle = \begin{cases} \dfrac{1}{\pi i}\dfrac{1}{x-y}, & x-y \text{ odd} \\ 0, & x-y \text{ even} \neq 0 \\ \frac{1}{2}, & x=y. \end{cases} \tag{2.17}$$

From (2.17) one finds that in the same limit:

$$\langle\sigma_x\sigma_y\rangle - \langle\sigma\rangle^2 = \begin{cases} -\dfrac{1}{\pi^2}\dfrac{1}{(x-y)^2}, & x-y \text{ odd} \\ 0, & x-y \text{ even} \neq 0 \\ \frac{1}{4}, & x=y. \end{cases} \tag{2.18}$$

Furthermore, if in the large-N limit one averages over all spin configurations occurring on the odd sites, one finds that the spins at the even sites become completely uncorrelated (and vice-versa the same thing).

At this point two comments on the form of the correlation functions (2.17) and (2.18) are in order. The first one concerns the origin of the oscillation between even and odd points and the second one is about the chiral anomaly. One would of course like to somehow identify the cellular automaton variable $\sigma_x - \langle\sigma_x\rangle$ with the fermionic current $\rho(x) = :\psi_x^\dagger\psi_x:$ in the continuum limit. It is however well known that this current only commutes up to the Schwinger term $\sim\delta'(x-y)$. This means that there should be an imaginary part in the correlation (2.18). We will see in the following that these two questions are related.

The crucial point is the compactness of momentum space (after going to the limit $N \to \infty$ we have also continuous momenta). Eq. (2.17) is now in p-space:

$$\langle \psi_p \psi_q^+ \rangle = \delta(p-q)\,\Theta(p). \tag{2.19}$$

The above correlation function has in fact two discontinuities, one at $p=0$ and one at $p=\pi$. The long-distance behavior gets therefore two contributions. $p=0$ gives $1/2\pi ix$ and the discontinuity at $p=\pi$ gives $-e^{i\pi x}/2\pi ix$ because of the different sign of the step and the shift by π in momentum space. These two contributions together characterize the long-distance behavior completely. The resulting oscillation is rather harmless if we go to the continuum limit. We introduce the dimensionful constant Λ and define the physical size of the momentum circle to be $2\pi\Lambda$. Letting now Λ go to infinity defines the continuum limit. In this process, we have to specify however, which states to keep. If we agree to keep only low-energy excitations of the field ψ, the contribution of the discontinuity at $\pi\Lambda$ is dampened by the standard ε-prescription for distributions by a factor $e^{-\varepsilon\Lambda}$. This vanishes if we perform the limit $\Lambda \to \infty$ before $\varepsilon \to 0$. This gives the correct two-point function for chiral fermions in the continuum limit,

$$\langle \psi_x^\dagger \psi_y \rangle = \langle \psi_x \psi_y^\dagger \rangle = \frac{1}{2\pi i}\,\frac{1}{x-y-i\varepsilon}. \tag{2.20}$$

Eq. (2.18) on the other hand is in Fourier space

$$\langle \hat\sigma_p \hat\sigma_q \rangle_c = \delta(p-q)\,|\,p\,|, \tag{2.21}$$

which does not give the standard current–current correlation function $p\Theta(p)$ in the continuum limit. Where does the negative p-part in (2.21) come from? Its origin lies again in the compactness of momentum space. Consider the contributions from the fermions according to Wick's theorem,

$$\begin{aligned}
\langle \hat\sigma_p \hat\sigma_q \rangle &= \int \mathrm{d}p'\ \mathrm{d}q'\ \langle :\hat\psi^\dagger_{p'-p}\hat\psi_{p'} :: \hat\psi^\dagger_{q'-q}\hat\psi_q : \rangle \\
&= \int \mathrm{d}p'\ \mathrm{d}q'\ \langle \hat\psi^\dagger_{p'-p}\hat\psi_{p'}\rangle \langle \hat\psi_p,\ \hat\psi^\dagger_{q'-q}\rangle \\
&= \int \mathrm{d}p'\ \mathrm{d}q'\ \Theta(-q')\Theta(q'-q)\delta(p'-p-q')\delta(p'-q'+q) \\
&= \delta(p+q)\int \mathrm{d}p'\ \Theta(p-p')\Theta(p').
\end{aligned} \tag{2.22}$$

Since the above step functions Θ have to be understood again in a periodic sense, we get an overlap also for $p \lesssim 0$ from the fermionic contributions near $p' = \pi$. This contribution will be dampened by a factor $e^{-\varepsilon \Lambda p}$; if we consider the ε-prescription to isolate the low-energy contributions of the fermions. Thus building $:\psi^\dagger\psi:$ and the continuum limit do not commute. The cellular automaton variable σ has fermionic contributions from both ends of the Dirac sea, while the fermionic current in the continuum limit has only the low-energy part. The crucial role played by the hamiltonian is therefore to give a selection principle on the states, which allow a continuum limit.

The model contains up to now only right-moving spins. Let us now attach a label "R" to the fields and operators corresponding to these spins, and subsequently add left-going particles, characterized by spins σ_x^{L} at each site x. We have the evolution law

$$\sigma_{x,t}^{\mathrm{L}} = \sigma_{x+1,t-1}^{\mathrm{L}}. \tag{2.23}$$

There are the corresponding Pauli matrices $\tau_x^{\mathrm{L}a}$, and now we perform the Jordan–Wigner transformation

$$\psi_x^{\mathrm{R}} = \left(\prod_{y=x-n}^{x-1} \tau_y^{\mathrm{R}3} \right) \otimes \tau_x^{\mathrm{R}-},$$

$$\psi_x^{\mathrm{L}} = \left(\prod_{y=x-n}^{x-1} \tau_x^{\mathrm{L}3} \right) \otimes \tau_x^{\mathrm{L}-} \prod_{y=-n}^{n} \tau_y^{\mathrm{R}3}, \tag{2.24}$$

where we made sure that also ψ_x^{L} anticommute with ψ_y^{R}.

The total hamiltonian replacing (2.10) is now

$$H = \frac{2\pi}{N} \sum_{p=-n}^{n} p\left(\hat{\psi}_p^{\dagger\mathrm{R}} \hat{\psi}_p^{\mathrm{R}} - \hat{\psi}_p^{\dagger\mathrm{L}} \hat{\psi}_p^{\mathrm{L}} \right) = \frac{2\pi}{N} \sum_{p=-n}^{n} p \hat{\psi}_p^\dagger \gamma^3 \hat{\psi}_p, \tag{2.25}$$

where γ^3 is the third Pauli matrix acting on the spinor $\binom{\psi^{\mathrm{R}}}{\psi^{\mathrm{L}}}$.

In the continuum limit this hamiltonian approaches

$$H \to \sum_x \mathscr{H}(x), \qquad \mathscr{H}(x) \to -i\psi_x^\dagger \gamma^3 \partial_x \psi_x, \tag{2.26}$$

the Dirac hamiltonian for massless non-chiral fermions.

The analysis of this model is no more difficult than the previous one. The left- and right-going sectors simply do not communicate with each other.

From a physical point of view this model is uninteresting. There is no interaction among left- and right-going particles. Indeed, any pattern of translationally invariant correlation functions among the leftgoers or among the rightgoers will

tend to be preserved in time because of the absence of interactions. In terms of quantum field theory: there is formally a wave function for each second-quantized particle, but the wave functions do not spread, and therefore there is no truly quantum mechanical behavior, yet.

In sect. 3 however we introduce a mass term. The wave functions for massive particles do spread in time, even in one space dimension, so then we do get truly quantum mechanical behavior. Furthermore, there will be interactions resulting into a non-trivial scattering matrix.

3. Simulation of a massive Dirac theory

In a quantum field theory fermions become massive if one adds a term

$$\psi_x^\dagger m\gamma^1\psi_x \tag{3.1}$$

to the hamiltonian density (2.25). It corresponds to

$$m\big(\psi_x^{\dagger\mathrm{R}}\psi_x^{\mathrm{L}} + \psi_x^\dagger\psi_x^{\mathrm{R}}\big), \tag{3.2}$$

which implies that a leftgoer turns into a rightgoer or vice versa. In fact, any kind of interaction at the fundamental level that could produce a transition among left- and rightgoers would ultimately produce such a mass term. Of course it breaks the separate conservation of the left and right chiral currents.

Hence our philosophy is that if we allow our cellular automaton to turn every now and then a rightgoer into a leftgoer or vice versa, this will result into a mass term of the kind (3.2). If this interaction is rare, the resulting mass term will be small.

So here is our new evolution law:
At every tick of our clock:
(i) the leftgoers move one step to the left and the rightgoers move one step to the right, as they did in sect. 2;
(ii) then the automaton checks at every site whether a leftmover is to be switched into a rightmover, or a rightmover into a leftmover. The switch is only made if a certain condition is met. The simplest example of such a condition is the following. At every site x we consider a set D_x of neighboring sites (for instance 3 neighbors at the left and 3 neighbors at the right). The condition is then

$$\sigma_x^{\mathrm{L}} = 1 - \sigma_x^{\mathrm{R}}, \qquad \sigma_y^{\mathrm{L}} = \sigma_y^{\mathrm{R}} \quad \text{for all } y \in \mathrm{D}_x. \tag{3.3}$$

In a rough approximation the probability for a switch at each site at each moment is 2^{-D}, where D is the dimension of D_x, so we can make the effect of this "mass correction" as small as we wish.

It should be clear that this latter revision of the evolution law makes a big difference. Our automaton is now highly non-trivial, and indeed suited for computer experiments. In many runs we saw that a system of this sort may turn into an apparently chaotic mode.

However, in our quantum field theoretical description, the new correction may be handled perturbatively. The perturbation expansion is with respect to the small parameter 2^{-D}.

After each time step the system evolves according to the evolution operator

$$\tilde{U} = U_1 U_0, \tag{3.4}$$

where U_0 is the unperturbed evolution operator:

$$U_0 = \mathrm{e}^{-iH_0}, \qquad H_0 = \frac{2\pi}{N} \sum_{p=-n}^{n} p \hat{\psi}_p^\dagger \gamma^3 \hat{\psi}_p. \tag{3.5}$$

In evaluating U_1 we encounter a little problem: the Jordan–Wigner transformation (2.24) determines the sign of ψ^{L} and ψ^{R} to depend on the number of rightgoers and leftgoers in all cells where a τ^3 contributes; this number is not constant. If we describe the switch by means of the operator

$$K_x = \psi_x^{\dagger \mathrm{L}} \psi_x^{\mathrm{R}} + \psi_x^{\dagger \mathrm{R}} \psi_x^{\mathrm{L}} = \psi_x^\dagger \gamma^1 \psi_x, \tag{3.6}$$

then the new state obtains a minus sign as phase factor in 50% of the cases.

It is not difficult however to convince oneself that this minus sign is harmless. If the evolution operator U switches the sign in front of the basis elements every now and then, this will not affect the probabilities $P(\sigma)$ that one is ultimately interested in. Again, we have a mathematical artifact of our calculational procedures that will not affect the ultimate results.

The eigenvalues of K_x are ± 1 and 0. So there is a basis in which

$$K_x = \mathrm{diag}(-1, 0, 1). \tag{3.7}$$

Here, the cases ± 1 correspond to the switch; 0 applies to the states where there are either two or zero particles at the site x.

To describe U_1, we want an operator that is 1 if there are two or zero particles, and performs the switch if there is one particle. Or:

$$V_x = \mathrm{diag}(-1, 1, 1) = \mathbb{1} + K_x - K_x^2 = \exp \frac{\pi i}{2} \left(K_x^2 - K_x \right). \tag{3.8}$$

Next, we want a projection operator P_x that is 1 if there are zero or two particles at site x, and else zero. This is the operator

$$P_x = \mathrm{diag}(0, 1, 0) = \mathbb{1} - K_x^2. \tag{3.9}$$

The operator U_x that decides to switch and performs the switch at the site x is now

$$U_x = (V_x)^{\prod_{y\in D_x} P_y} = \exp\left(\frac{\pi i}{2}\left(K_x^2 - K_x\right)\prod_{y\in D_x}\left(\mathbb{1} - K_y^2\right)\right). \tag{3.10}$$

The different operators K_x all commute with each other. Therefore we can write

$$U_1 = \prod_x U_x = \exp\sum_x\left(\frac{\pi i}{2}\left(K_x^2 - K_x\right)\prod_{y\in D_x}\left(\mathbb{1} - K_y^2\right)\right). \tag{3.11}$$

Our hamiltonian $\tilde{H}$ will be defined by

$$\tilde{U} = U_1 U_0 = \mathrm{e}^{-i\tilde{H}}, \tag{3.12}$$

but it will be more convenient to use

$$U = U_0^{1/2} U_1 U_0^{1/2} = \mathrm{e}^{-iH}; \tag{3.13}$$

H and $\tilde{H}$ are unitarily equivalent.

4. Calculation of the mass and interaction terms

For all states that we are interested in, U_1 may be considered to be the exponent of a "small" quantity. How can we see that the exponent in (3.11) is small?

At this point we will decide to consider only the vacuum of the unperturbed, massless theory and its lowest-energy excitations. It is this class of states for which all matrix elements of the exponent in (3.11) will be small. To see this, we have to normal-order all operators in there. Normal ordering means that, by using the commutation rules, all operators that create a particle are shifted to the left and all annihilation operators to the right. The creation operators are

$$\hat{\psi}_p^\dagger \quad (p > 0) \quad \text{and} \quad \hat{\psi}_p \quad (p \leqslant 0) \tag{4.1}$$

and their hermitian conjugates are the annihilation operators.

One writes

$$
\begin{aligned}
:AB: &= -BA \quad \text{if } A \text{ is an annihilation operator} \\
&\qquad\quad \text{and } B \text{ a creation operator,} \\
&= AB \qquad \text{otherwise.}
\end{aligned}
$$

(the minus sign occurs of course as long as we work with fermionic operators. Similarly one can normal-order larger products,

$$
:ABC\ldots:.
$$

Normal ordering is a way to be economical. A matrix element of a normal-ordered product of N operators is non-vanishing only if the bra and the ket together contain at least N particles.

We have

$$
\begin{aligned}
\hat{\psi}_p^\dagger \hat{\psi}_q &= :\hat{\psi}_p^\dagger \hat{\psi}_q: + \delta_{pq}\theta(-p), \\
\hat{\psi}_p \hat{\psi}_q^\dagger &= :\hat{\psi}_p \hat{\psi}_q^\dagger: + \delta_{pq}\theta(p), \\
\psi_x^\dagger \psi_y &= :\psi_x^\dagger \psi_y: + f(x-y), \\
\psi_x \psi_y^\dagger &= :\psi_x \psi_y^\dagger: + g(x-y),
\end{aligned}
\tag{4.2}
$$

with in the large-N limit (z integer):

$$
\begin{aligned}
f(2z) &= \tfrac{1}{2}\delta_{z0}, \\
f(2z+1) &= i/\pi(2z+1), \\
g(z) &= f^*(z).
\end{aligned}
\tag{4.3}
$$

Larger normal products can be obtained by applying (4.2) successively:

$$
\psi_x^\dagger \psi_y \psi_z = :\psi_x^\dagger \psi_y \psi_z: + f(x-y)\psi_z - f(x-z)\psi_y, \tag{4.4}
$$

etc.

We find in (3.11),

$$
\begin{aligned}
K_x^2 - K_x &= :K_x^2 - K_x + \tfrac{1}{2}\mathbb{1}:, \\
\mathbb{1} - K_y^2 &= :\tfrac{1}{2}\mathbb{1} - K_y^2:.
\end{aligned}
\tag{4.5}
$$

To work out the product in (3.11) we have to normal-order also the different factors. This becomes trivial if D_x only contains neighbors y at an even distance from x, because then $f(x-y)=0$. In that case we find

$$U_1 = e^{-iV}, \qquad V = \sum_x V_x, \tag{4.6}$$

with

$$V_x = -\frac{\pi}{2} :\left(K_x^2 - K_x + \tfrac{1}{2}\right) \prod_{y \in D_x} \left(\tfrac{1}{2} - K_y^2\right):$$

$$= 2^{-D-1}\pi\left(:\psi_x^\dagger \gamma^1 \psi_x : + \sum_{y \in D_x} :\left(\psi_y^\dagger \gamma^1 \psi_y\right)^2 : - :\left(\psi_x^\dagger \gamma^1 \psi_x\right)^2 : + O\left(:\left(\psi^\dagger \psi\right)^3 :\right)\right). \tag{4.7}$$

Note that it is not at all necessary to take only the even distances in the set D_x; there are objections one can make against choosing D_x this way (see later). We only did this to get the simple expression (4.7). In the other cases we just get some extra terms due to normal ordering.

Now we must find H such that

$$e^{-iH_0/2}\, e^{-iV}\, e^{-iH_0/2} = e^{-iH}. \tag{4.8}$$

According to the Baker–Campbell–Hausdorff formula H can be expressed as a series whose terms are H_0, V and commutators of these:

$$H = H_0 + V + \tfrac{1}{24}[H_0, [H_0, V]] + \tfrac{7}{5760}[H_0, [H_0, [H_0, [H_0, V]]]] + \ldots$$

$$+ O(V^2), \tag{4.9}$$

where the terms of order V^2 start as

$$\tfrac{1}{12}[V, [H_0, V]] + \ldots . \tag{4.10}$$

(If H was not defined symmetrically as in (5.8) one would get more commutator terms in (4.9).)

Now we claim that for a good understanding of the large-scale behavior of this theory all higher-order terms in (4.9) are relatively unimportant.

The series (4.10), quadratic in V, is of order 2^{-2D} since V is of order 2^{-D}. But also the higher commutators linear in V in the series (4.9) are small corrections. Note that

$$[\psi^\dagger A \psi, \psi^\dagger B \psi] = \psi^\dagger [A, B] \psi, \tag{4.11}$$

so that

$$\left[H_0, \psi^\dagger\gamma^1\psi\right] = \psi^\dagger\left[\gamma^3 p, \gamma^1\right]\psi = i\psi^\dagger\gamma^2 p\psi, \tag{4.12}$$

and

$$\left[H_0, \left[H_0, \psi^\dagger\gamma^1\psi\right]\right] = \psi^\dagger\gamma^1 p^2\psi. \tag{4.13}$$

Thus, the higher commutators contain higher derivatives of ψ. There are two ways to understand why such terms may be neglected. One is by noticing that we are interested in low-energy excitations around the vacuum state. These correspond to particles with small momenta p. Hence the operator (4.13) acting on them is small. Alternatively, one may view these operators as what is called *marginal* couplings in lattice quantum field theories. They are non-renormalizable. Their strengths are relatively small even at the lattice scale. If we scale to a low-energy domain their effects become negligible.

In the same vein, the terms of order $(\psi^\dagger\psi)^3$ and higher in (4.7) may be neglected because they are marginal. The dominant terms in the hamiltonian describing the low-energy domain are

$$H = i\psi^\dagger\gamma^3\partial_x\psi + m\psi^\dagger\gamma^1\psi + g\left(\psi^\dagger\gamma^1\psi\right)^2, \tag{4.14}$$

where with our choice for D_x

$$m = 2^{-D-1}\pi, \qquad g = 2^{-D-1}(D-1)\pi. \tag{4.15}$$

Indeed, this is a massive Dirac theory with a weak interaction among the fermions. The terms in (4.14) are normal ordered with respect to the massless vacuum. This means that in a Feynman diagram expansion for the scattering matrix of the theory one still has vacuum bubble diagrams to take into account.

Note that our theory is well defined as a perturbation expansion in the small parameter 2^{-D-1}. All terms that we neglect so far can be corrected for in terms of this expansion.

But if one leaves the domain where this expansion is expected to make sense (the low-energy, large-distance domain), then no convergence of the series is guaranteed. What this means for the cellular automaton itself is not entirely clear. A problem is that in the original system *energy* can only be defined modulo 2π. To perform a translation over fractional amounts of time is really only a mathematical artifact, void of any rigorous physical meaning. Does this mean that non-perturbative effects can violate energy conservation by integer multiples of 2π? This is not entirely clear to us. It would mean that even if we start with a low-energy configuration, the system may run away from it. Or: if we start with a configuration with the correlation functions typical for the quantum field theoretical vacuum or

small excitations away from that, these correlations may perhaps not stay forever but dissipate away.

In the real world there is a quite different mechanism that protects energy in being exactly conserved: the coupling to gravity. To incorporate anything like general coordinate invariance (in particular with respect to the time coordinate) is a tricky thing to try in a cellular automaton. It could be that without the gravitational force no exactly conserved energy is possible in a cellular automaton.

5. Numerical simulation

This section contains a discussion of the numerical simulations we performed to treat our model and the conclusions to be drawn from them.

The problem for determining the correlation functions of the cellular automaton variables is, of course, that one does not know the vacuum state in general. An arbitrary state may contain arbitrarily high energy excitations. Some kind of cooling mechanism, which drives an arbitrary state to the vacuum would be extremely useful. In the real world, the expansion of he universe does such a job. One might therefore try to invent an expanding version of the automaton, in which at each step some new cells are added. In principle this is a possibility. In practice however there turned out to be a problem. In our models energy is conserved only modulo 2π. This may imply that there can be energy production in units of 2π. Because of this we found that an expanding cellular automaton rapidly heats up. This is thus not a very promising approach.

There is another way to cool at least a given finite region of the interacting theory. Suppose that we switch on the interaction in a region of space with size L. If there exists a local hamiltonian density for the interacting theory, we can join it to the free hamiltonian density (2.25) outside L. Outside we know however how the vacuum looks. In this way we can control the energy-flow into L, i.e. it is zero if the state outside is the free vacuum. We can actually start with the free vacuum as initial state. With respect to the interacting vacuum inside L this state has a lot of excitations, which should however dissolve gradually into the free vacuum outside. This would effectively cool down the interacting region. Viewed from the outside, after an initial burst of energy, the system should again relax to the vacuum state. The assumption of a local hamiltonian density is crucial here, since it allows to consider the inside and outside regions separately.

In this approach it is also not quite clear whether there will be energy production in units of 2π, but at least we have a good idea of how to cool the system at the sides. So this was what we decided to study numerically in more detail. The first thing to do is to generate the free Dirac vacuum according to the Boltzmann weight (2.15). The total number of participating configurations is however far too big ($O(2^N)$, with N the total number of cells) to be treated exactly

by any computer. We have to approximate the canonical ensemble by a Monte Carlo procedure. Recall that according to (2.13), the vacuum state is a superposition of our basis vectors $|\sigma_1, \sigma_2 \ldots \sigma_N\rangle$ with the corresponding weight and phase. As explained above, we shall be interested only in the correlation functions of the σ-operators and therefore the relative phases of the members of the vacuum superposition will not matter as they cancel in expressions like $\langle \sigma \ldots \sigma \rangle$. This fact gives us the possibility of treating the vacuum state as a statistical ensemble.

Next we create a separate set of cells which represents the interaction region (with size L) and which will be called shortly the inside region in distinction with the region where the free vacuum was created. The latter we call outside region. The evoluton of the content of the cells in the inside region is according to the

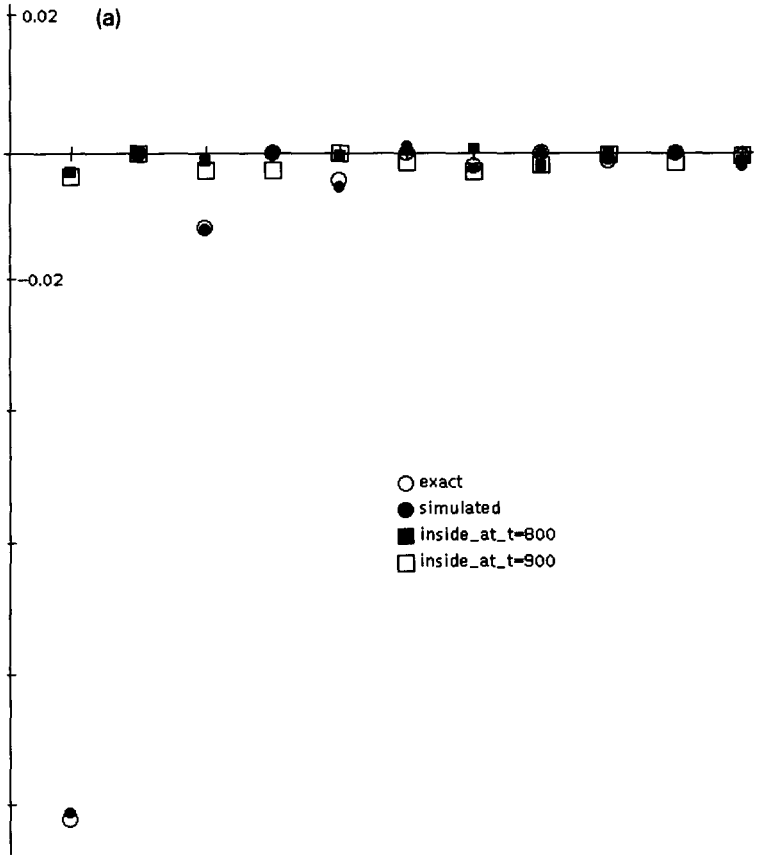

Fig. 1. Results from the simulation experiment with $L = 96$ and relaxation time 900. (a) The two-point correlation function inside the interaction region. (b) The left–left correlation function measured outside the interaction region. The total size of the automaton is $N = 901$ cells and the number of Monte Carlo samples is 10^7. The initial content of the interaction region is taken randomly for each MC sample.

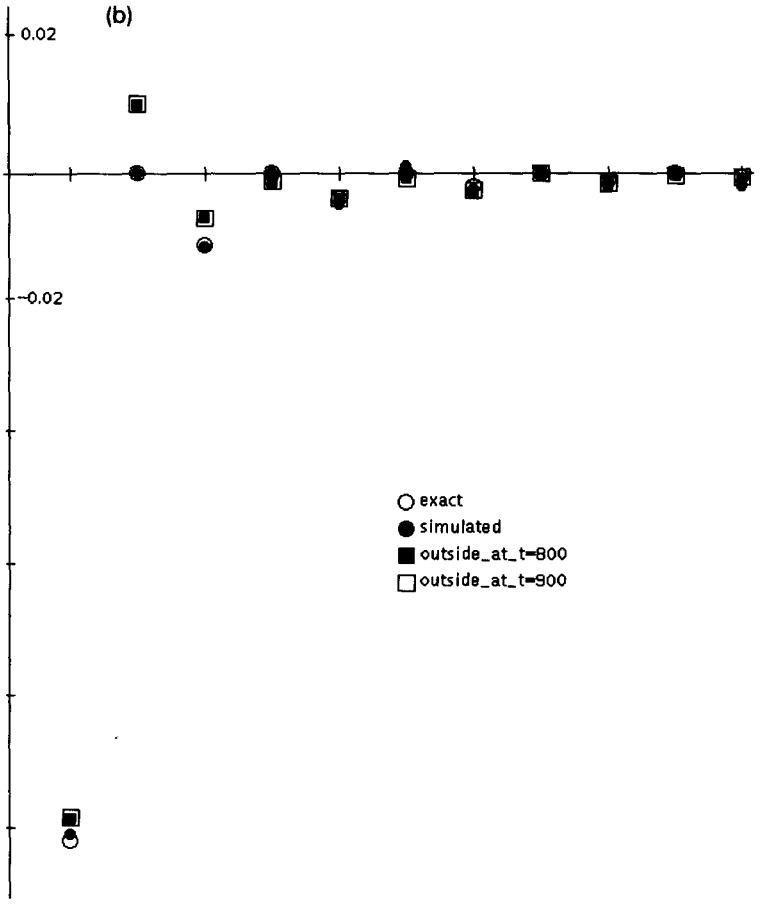

Fig. 1. (continued).

interacting rule. This interaction region is open on both sides, so at each time step we must "feed" it from the left and from the right with right and left movers correspondingly. To simulate the free vacuum outside we feed the interaction region with the generated Dirac vacuum. For this situation it should actually not matter, how the initial state looks inside the interaction region. We then measure the correlation functions before this evolution, inside and outside L after the evolution for a certain relaxation time. This gives us information about the quality of the simulation of the free vacuum, the correlation of the σ's in the putative interacting vacuum and the relaxation outside respectively.

Let us now mention some technical details of the Monte Carlo procedure. We use a standard Metropolis algorithm. Since we have to conserve the total number of plus spins, we propose an exchange in position of a random plus–minus pair. If the ratio of the Boltzmann factors of the new over the old configuration is bigger

than one, we accept the new configuration; if it is smaller than one, we accept it with the probability given by this ratio. We obtained the best results when we took this output configuration and perform on it a random rotation.

The main quantity of all our computer experiments is the two-point connected correlation function $\langle \sigma_x \sigma_y \rangle$. Since we can compare the measured two-point correlation function in the free region with the exact one, we have a direct control over the accuracy of the simulation. It turned out that to get an accurate third digit, we needed about ten million configurations for the size N of the automaton of the order of a few hundred. The computation time for this is of the order of a few days on a DEC station 5000/200. This poses an upper bound on the feasibility of our method, which is actually sufficient to get outside the boundary effects only for the ultimate case when the interactions described in sect. 4 involve only the

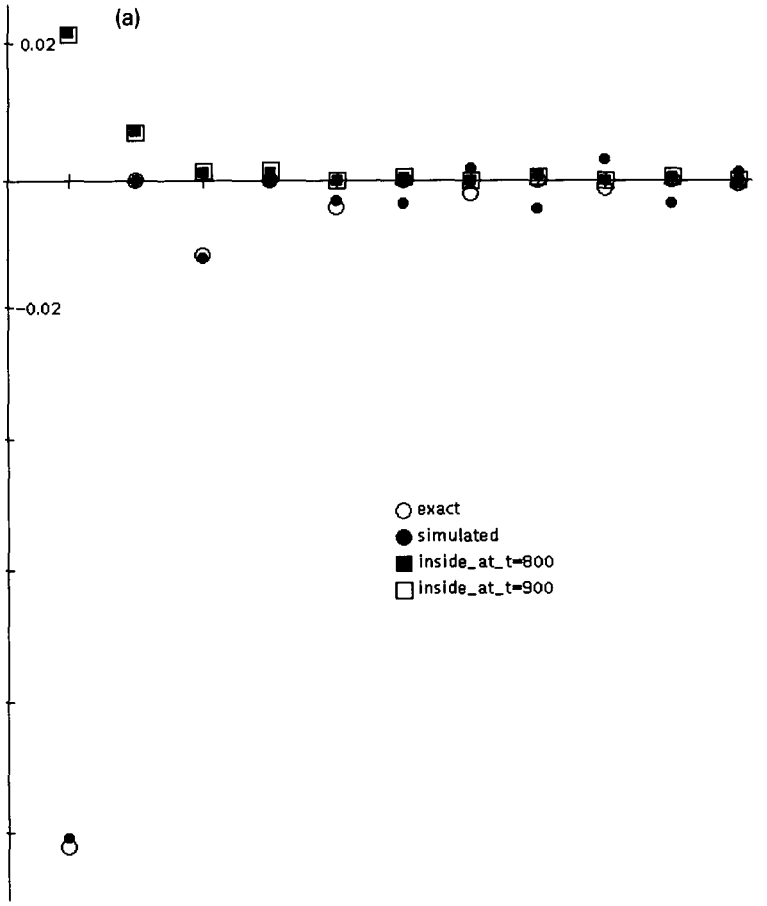

Fig. 2. The same as fig. 1 except that initially the content of the interaction region had short-range correlations.

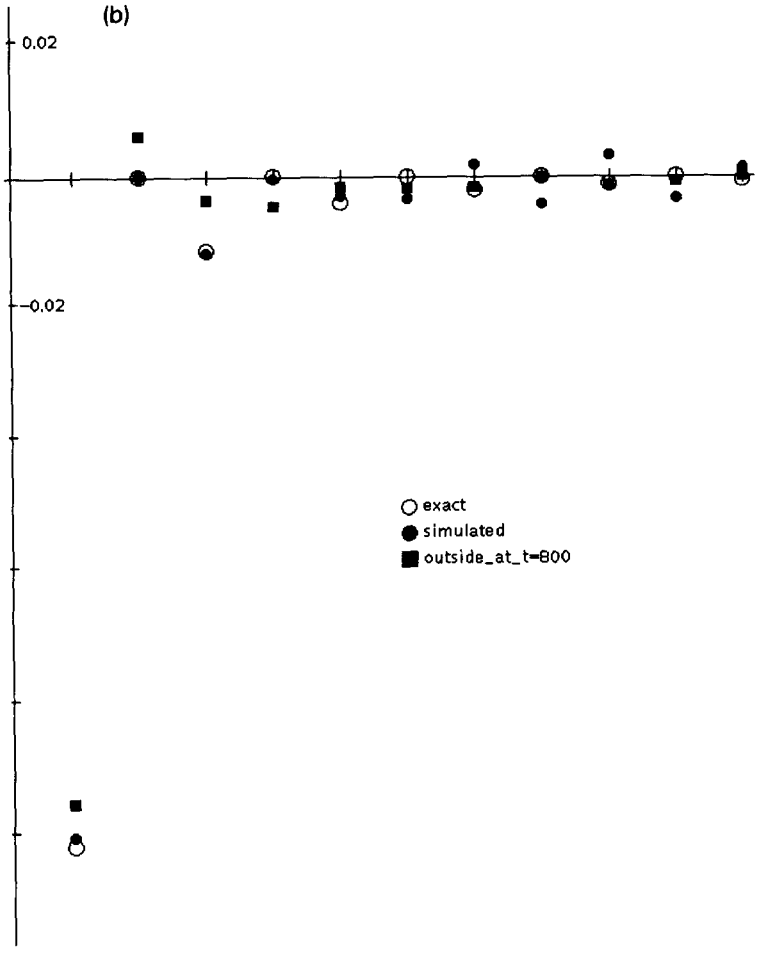

Fig. 2. (continued).

closest two neighboirs of each cell (therefore $D = 2$). All our results concern only this case.

Figs. 1a, b summarize the results of a typical such simulation. Black and white points correspond to the simulated and theoretical two-point correlation functions at distances 1, 2, etc. The coincidence of these points indicates the quality of our Monte Carlo simulation. The black and white squares represent the measured two-point function (inside the interaction region in fig. 1a and outside in fig. 1b) for two values of the relaxation time. Their coincidence is indicative for a relaxation in both regions. Actually it turns out that the relaxation occurs much faster outside.

We now discuss the results obtained from our simulation experiments. The clearest signal that something went wrong is presented by the correlations outside.

They relax to stationary values, which are however not the expected free correlations. There is a peak at roughly half the value of D_x. This is clearly a significant effect. Since the one-point function relaxes to the vacuum value, there is no charge produced. The only other physical observable is energy. That means that there must be a constant energy production inside the massive region, the system does heat up! This situation seems to be rather generic for this type of automata. We did some runs with different types of interactions, i.e. when the left–right exchange in a given cell is performed when there is an unequal left–right content on both sides of this cell. There the situation seems to be even worse, the correlations relax to approximately zero. In fact, the approximate restoration of the free correlations outside is due to a reflection effect (see below). The correlation functions inside the massive regions are strongly damped, actually stronger than could be expected

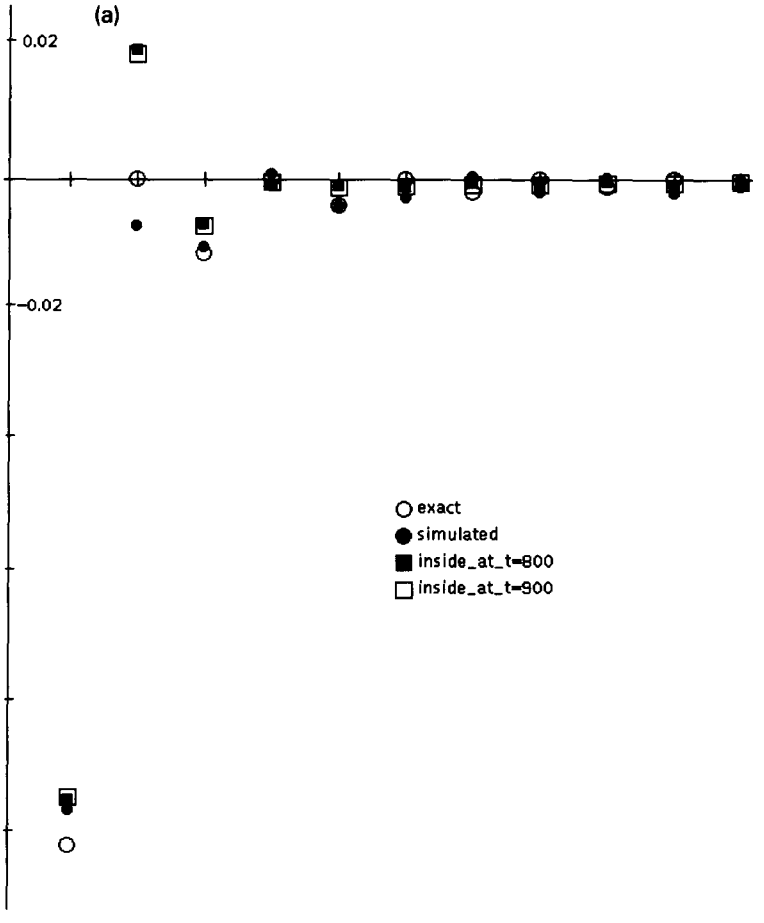

Fig. 3. The same as fig. 1 except that the initial content of the interaction region was taken to be the corresponding piece of the free vacuum.

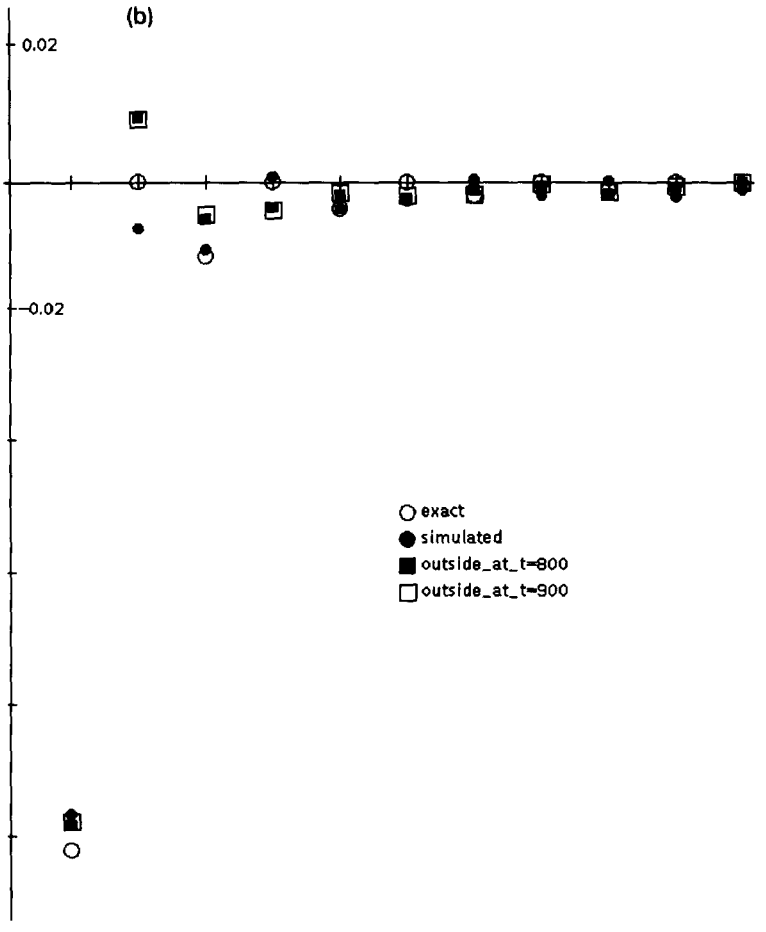

Fig. 3. (continued).

from an exponential damping with a mass of the order of the estimated value $O(2^{-D})$ (see (4.15)). An exponential decay is however rather difficult to verify, since it requires knowledge of the correlation for large distances. This requires large samples to get the needed accuracy, since one has to avoid the effects of the boundary and a too small relaxation time. Both these could introduce fake correlations.

A look at fig. 6a gives a intuitive insight of what happens in this particular slice of our Monte Carlo simulation (the latter comprises superimposed millions of these pictures). Each even (odd) dot in fig. 6a represents an occupied cell by a left (right) goer. We see that inside the interaction region self-created thick walls are reflecting everything. That suggests that inside correlations will "remember" the initial setup. at the same time the approximate similarity between the outgoing

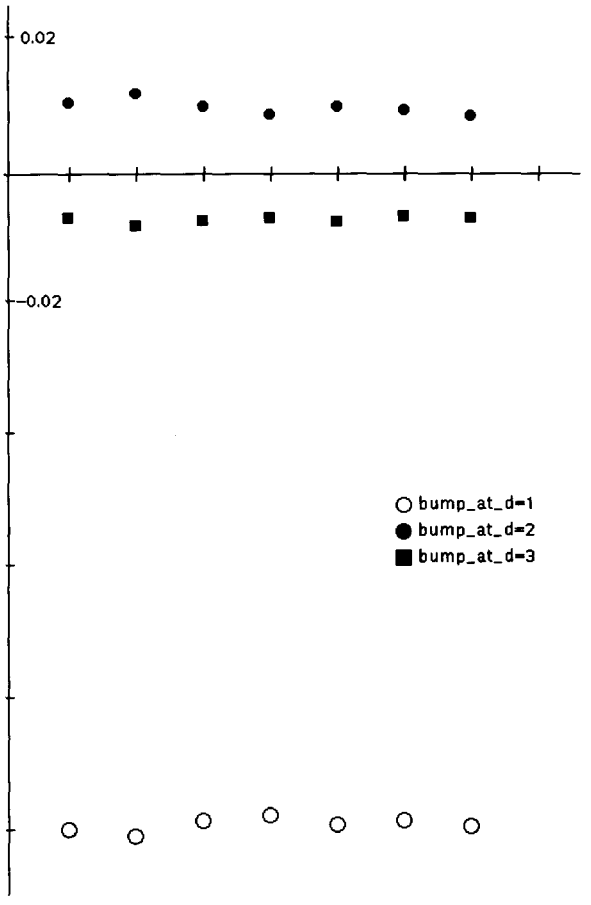

Fig. 4. Three characteristic values of the two-point correlation function outside the interaction region taken from computer experiments with different sizes of this region and different relaxation times. This is to illustrate the independence of these values on the corresponding parameters. The range of L is from 51 to 196 cells.

correlations and the free one is due to pure reflection from any of the inside walls. This is more precisely illustrated on fig. 1–3. On these figures we show the simulation results for different initial setups in the interaction region. Fig. 1a depicts the inside correlations obtained with a random initial while fig. 2a corresponds to short-distance correlated initial values. Finally fig. 3a shows the simulation result for the free vacuum initially in the interaction region. We see therefore that the final correlations in all these cases are different and in some sense preserve the information set initially. At the same time the corresponding outside two-point correlations, as shown on figs. 1b, 2b and 3b are very similar. More rigorously this is shown on fig. 4 where we present three different values of the two-point correlation function in the outside region (taken at distances 1, 2 and 3)

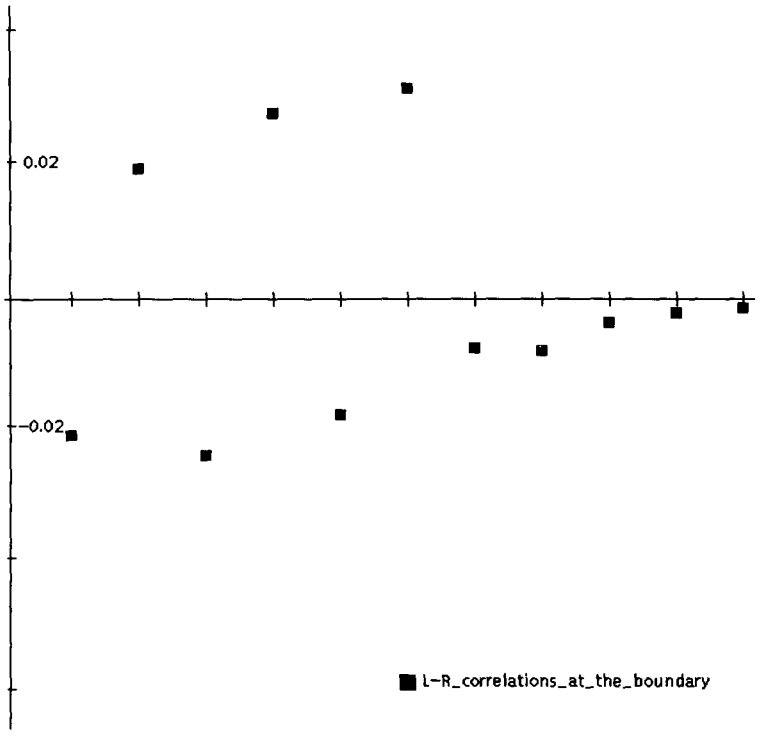

Fig. 5. Two-point left–right time–time correlation function measured in a point close to the border of the interaction region.

obtained from different Monte Carlo experiments with different sizes of the interaction region. The values coincide within the precision, which confirms the conclusion that the reflection effects dominate.

The reflection phenomena are investigated quantitatively by measuring $\langle \sigma_{\mathrm{L}}^{x,t} \sigma_{\mathrm{R}}^{x,t-s} \rangle$, the left–right connected two-point time–time correlation function in the same space point at the border of the interaction region. The results are depicted in fig. 5. where the horizontal axis represents s, the time delay, and the vertical the normalized connected two-point correlation function. The high peaks correspond to reflections (and thus self-correlations) from different walls inside the region. The deep negative values are due to the anti-correlation of the reflected free-vacuum at odd distances.

As stated above, we also considered other forms of left–right interactions. Specifically, fig. 6b shows the evolution based on the similar rule as the above except that the left–right flip occurs if the neighboring sites are unequal. We see no walls inside, but the left–left correlations outside the interaction region relax to zero and therefore make this case even worse. In conclusion we must say that the method of relaxation in a finite region does not produce the correlations expected

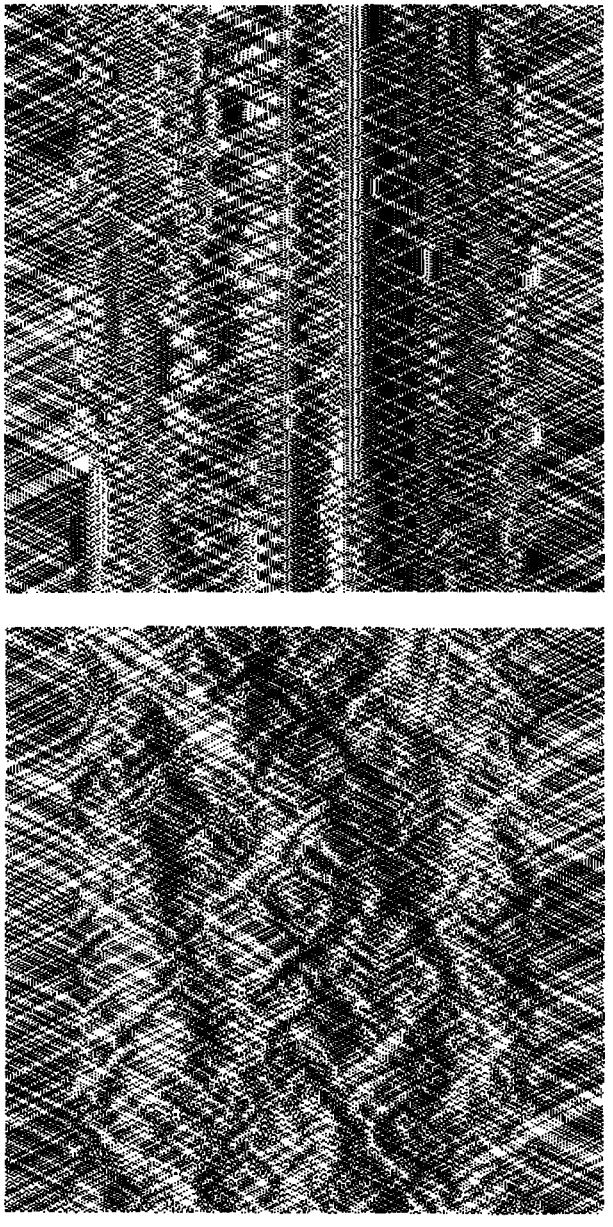

Fig. 6. Two-dimensional segment of the time (vertical, downwards) evolution for the cellular automata with equality checks (a) and unequality checks (b) at neighboring sites inside the interaction region. The interaction region is bordered on both sides by clearly visible free regions which receive random inputs.

from field theoretic considerations. It is not clear at this stage whether this is a failure of the whole cellular automaton approach or this is an artefact of our particular implementation. It could be that there still exists a satisfactory local

hamiltonian density, but of cellular automaton type only deep inside and far outside the interaction region. This would mean that around the boundaries one has to take into account also the phases of the individual configurations. In such a case the use of a cellular automaton dynamics for finding the interactive vacuum is extremely limited. Alternative methods other than the ones described here are lacking so far, though we have certain ideas to be described later.

K.I. would like to thank FOM for financial support. S.K. thanks the Institute for Theoretical Physics at the University of Utrecht for the hospitality.

References

[1] For cellular automata see:
E. Fredkin and T. Toffoli, Int. J. Theor. Phys. 21 (1982) 219;
T. Toffoli, Int. J. Theor. Phys. 21 (1982) 165; Physica D10 (1984) 117;
R.P. Feynman, Int. J. Theor. Phys. 21 (1982) 467;
S. Wolfram, Physica D10 (1984) 1;
N.H. Margolus, Physica D10 (1984) 81;
S. Wolfram, Rev. Mod. Phys. 55 (1983) 601
[2] G. 't Hooft, J. Stat. Phys. 53 (1988) 323; Nucl. Phys. B342 (1990) 471